Improved State Estimation in Quadrotor MAVs

A Novel Drift-Free Velocity Estimator

By Dinuka Abeywardena, Sarath Kodagoda, Gamini Dissanayake, and Rohan Munasinghe

Quadrotor microaerial vehicles (MAVs) are simple robotic platforms with regard to their construction. In their basic form, they are no more than two counterrotating propeller pairs attached symmetrically to a rigid crosslike frame, along with the means to control the speed of each individual propeller. This symmetric design has enabled the quadrotor to become a simple but powerful vertical takeoff and landing aerial platform popular among the robotics community.

With this simplicity comes the burden of controlling motion in three-dimensional (3-D) space using just four actuators. The underactuated and coupled dynamics of the quadrotor make it nearly impossible for a human pilot to gain control over it, unless a well-tuned control system is used. Such a control system is also vital if autonomy is a goal, as is the case with most MAVs. Estimates of controlled states and their derivatives are essential for any control system, and where those estimates are accurate and frequent in time, it has been demonstrated that quadrotors have extreme maneuverability and agility [1].

With regard to design, however, the MAVs are limited in their payload capacity and, with this limitation, obtaining accurate and fast state estimates becomes a challenge. For example, microelectromechanical systems (MEMS) inertial sensors can provide fast but coarse state estimates [2], whereas exteroceptive sensors, such as lasers and cameras [3], render more accurate state estimates, albeit at a slower rate. Attempts to merge these two sensing domains are frequent in the MAV literature [4], [5], and an application of similar ideas to quadrotors was presented in [6].

Digital Object Identifier 10.1109/MRA.2012.2225472

Date of publication: 10 June 2013

One aspect common to most MAV state estimators is their use of inertial sensors. Typically, gyroscopes, accelerometers, and magnetometers are used for the purpose of attitude estimation [7]. Based on a long history of research in inertial navigation systems, the sensor fusion algorithms usually employed for this task make use of the equations of motion of the sensing unit in 3-D space. The main advantage of this approach is that these generic estimators are specific only to the sensor package geometry and can be used independently of the platform on which the sensors are mounted. However, they fail to exploit the dynamics of the vehicle under consideration in the estimation process, leading to a potentially suboptimal result. The value of using specific dynamic characteristics of the vehicle has been reported in the case of land vehicles [8] and air vehicles [9]. Similarly, in this article we demonstrate that the influence of blade flapping in a quadrotor leads to a set of dynamic equations that can aid state estimation using inertial sensors.

Background and Motivation

The MAV attitude estimators that fuse the gyroscope and the accelerometer measurement using generic algorithms are frequently reported in the literature [10], [7], [2]. These algorithms operate by fusing measurements of a triad of body-mounted gyroscopes and accelerometers. The gyroscope measurements are a source of high-frequency attitude rate information, but alone they are not sufficient for the drift-free attitude estimation due to bias and various other forms of noise present in a typical low-cost sensor. The attitude estimators for MAVs overcome this issue by assuming that accelerometers predominantly measure gravitational acceleration and are thus capable of providing low-frequency information about the MAV orientation with respect to gravity. When the vehicle accelerations are significant, as in the case of a

1070-9932/12/$31.00©2012IEEE

quadrotor, this assumption does not hold [11]. Furthermore, such estimators are incapable of drift-free velocity estimation, as they can only be generated by integrating noisy accelerometer measurements. To complicate matters even further, accelerometer measurements need to be compensated for gravity before this integration, and such compensation requires an accurate attitude estimate. As mentioned before, one promising way to overcome these deficiencies is to examine the behavior of the MAV in question to identify suitable characteristics that would assist the estimation process.

Martin et. al. [12] have analyzed the behavior of a quadrotor MAV in detail and also presented the equations describing measurements of an accelerometer mounted on a quadrotor. Their results motivated us to reformulate the state estimators for quadrotors and to redesign them, considering the true sensor behavior as opposed to conventional vehicle-independent assumptions. In addition to improving the accuracy of the attitude estimate, the design presented here provides a drift-free estimate of the horizontal components of translational velocity of the quadrotor. Recently, a similar idea was presented in [13] where two separate nonlinear complementary filters were utilized to estimate the attitude and the velocity of a quadrotor MAV. The filter formulation presented in this article is different from [13], and we also present experimental results validating the concept. The velocity estimates thus derived are of critical importance to control and navigational tasks of a quadrotor, as will be discussed in our concluding remarks.

Quadrotors: What Makes Them Unique?

A thorough derivation and analysis of the quadrotor dynamics can be found in [12] and [14]. Rather than reiterating the derivation, here we aim to briefly summarize the important equations and to provide an intuitive description of the most salient features of the dynamic behavior that makes quadrotors a unique MAV.

Let $\{E\}$ be the earth-fixed inertial frame, and a vector $[x\ y\ z]^T$ denotes the position of the center of mass of the quadrotor expressed in $\{E\}$ (see Figure 1). Let $\{B\} \equiv [b_1\ b_2\ b_3]^T$ be a body-fixed frame positioned at the center of mass of the quadrotor.

The orientation of $\{B\}$ with respect to $\{E\}$ is defined using a cumulative rotation of Euler angles ψ (yaw), θ (pitch), and ϕ (roll), in that order, around b_3, b_2, and b_1, respectively. R is defined as the rotational transformation matrix from $\{B\}$ to $\{E\}$. The kinematic equation relating the instantaneous angular velocity $\Omega \equiv [\omega_x\ \omega_y\ \omega_z]$ of $\{B\}$ with respect to $\{E\}$ to Euler rates can be expressed as

$$\begin{bmatrix} \dot{\phi} \\ \dot{\theta} \\ \dot{\psi} \end{bmatrix} = \begin{bmatrix} 1 & \tan\theta\sin\phi & \tan\theta\cos\phi \\ 0 & \cos\phi & -\sin\phi \\ 0 & \sin\phi/\cos\theta & \cos\phi/\cos\theta \end{bmatrix} \begin{bmatrix} \omega_x \\ \omega_y \\ \omega_z \end{bmatrix}. \quad (1)$$

The equation describing the evolution of translational motion of the quadrotor as derived in [12] is of special interest to the estimator design that will be presented in following sections.

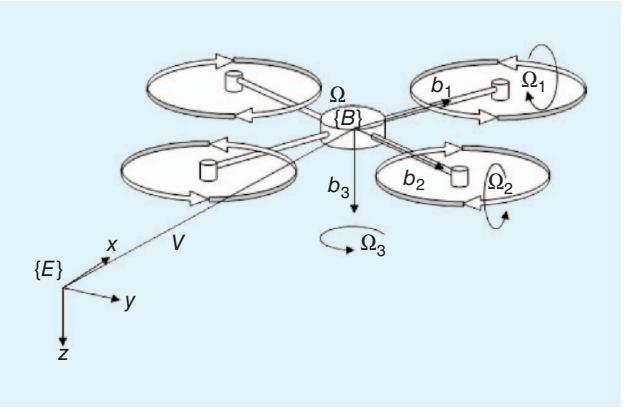

Figure 1. Coordinate frame definitions for the quadrotor dynamic model.

$$m\dot{\mathbf{V}} = m\mathbf{g} - k_T \sum_{i=1}^{4} \omega_i^2 \mathbf{b}_3 - \lambda_1 \sum_{i=1}^{4} \omega_i \tilde{\mathbf{V}}, \quad (2)$$

where $\mathbf{V}$ is the velocity of {B} as observed from an inertial frame, $\mathbf{g}$ is the gravity vector, k_T is the thrust coefficient of propellers, λ_1 is a positive coefficient known as the rotor drag coefficient, ω_i is the rotational velocity of the ith rotor, where $i \in \{1, 2, 3, 4\}$, $\tilde{\mathbf{V}}$ is the projection of $\mathbf{V}$ on to the propeller plane, and m is the mass of the quadrotor.

Equation (2) sheds light on two key aspects of the quadrotor. The first and the most obvious is the fact that the thrust force is perpendicular to the propeller plane and thus has no effect on the motion along that plane. Second, and more importantly, we see the presence of a force, which is proportional to the translational velocity of the quadrotor. For an intuitive description of this force, we refer readers to Figure 2, which shows a cross section of a quadrotor in flight, and we provide a simplified explanation of the origin of this force.

Figure 2 shows a quadrotor in a hypothetical state where it has tilted sideways to initiate a translation in a horizontal direction, but immediately before it gains any translational motion. At this point, thrust from propellers and gravity are the only forces acting on our simplified quadrotor model. In this particular state, the thrust force generated from the propellers is perpendicular to the propeller plane.

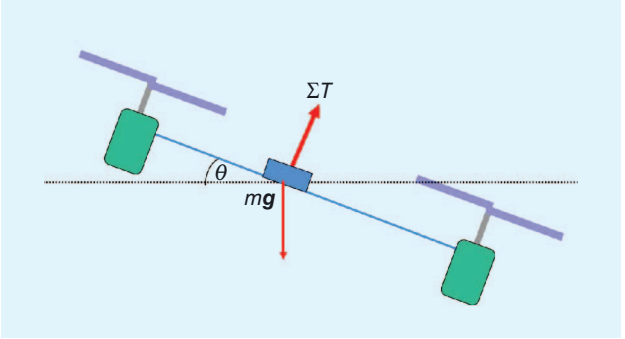

Figure 2. A schematic of a quadrotor immediately after tilting sideways, but before it starts moving. ΣT is the summation of propeller thrusts and corresponds to the second term in (2).

The state depicted in Figure 2 is hypothetical in the sense that even the slightest tilt of the quadrotor will induce translational motion. Figure 3 shows a more realistic situation in which the quadrotor moves right with a nonzero velocity. For a propeller with two blades, we can now identify a retreating and an advancing blade, as shown in blue and green, respectively, in Figure 4. The velocity of the advancing blade with respect to free air is higher than that of the retreating blade due to the translational velocity of the whole quadrotor. This creates a force imbalance between the two blades of the same propeller and causes the blades to flap up and down as they rotate. Blade flapping forces the propeller to rotate out of plane, and the flapping angle of a blade is at a maximum just before it transitions from the advancing state to the retreating state or vice versa. As shown in Figure 3, blade flapping causes the thrust force of the propeller to be tilted in a direction, which opposes the motion of the quadrotor. As the amount of blade flapping is dependent on the translational velocity of the quadrotor, the component of the thrust force along the body plane is also a function of that velocity. The last term in (2) models the impact of this component of the thrust force on the translational motion of the quadrotor. If one places an accelerometer on the quadrotor with its sensing axis parallel to the propeller plane, the accelerometer will measure a force that is roughly proportional to the velocity of the quadrotor along the same axis. In fact, in the next section, it is shown that this is the only significant force that the accelerometer will sense. [Interestingly, (2) ignores the aerodynamic drag experienced by a body moving through the air, which is usually a function of the square of the velocity. This can be justified for the quadrotor MAVs that move at relatively low speeds.] This is the unique characteristic of the quadrotor MAVs that will later be exploited to the benefit of the state estimator.

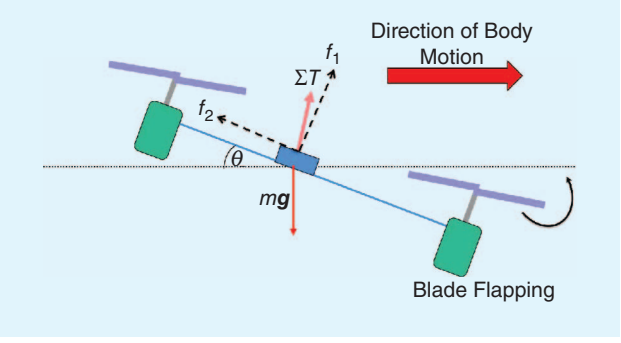

Figure 3. After tilting, the quadrotor starts moving sideways, f_1 and f_2 are the orthogonal components of ΣT.

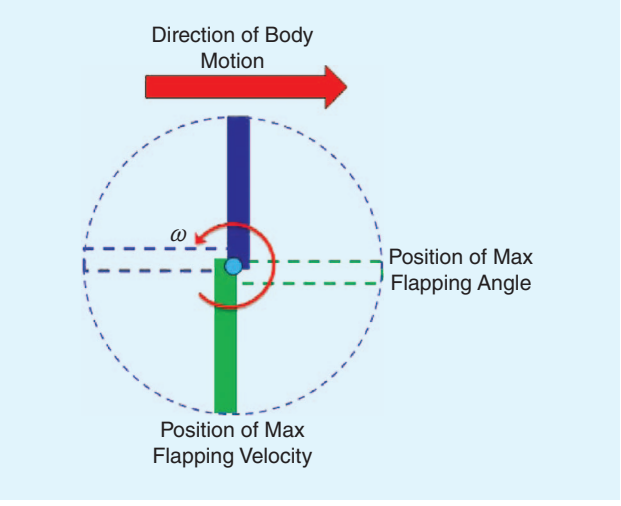

Figure 4. As the propeller blades rotate, flapping is determined by their position with respect to the direction of motion of the propeller as a whole.

We rewrite (2) using ${}^b\mathbf{V}$ (i.e., $\mathbf{V}$ in $\{B\}$ frame) to facilitate the estimator design. After neglecting the second-order terms that appear because of coordinate frame transformation, the first two components of ${}^b\dot{\mathbf{V}} \in \{{}^b\dot{v}_x, {}^b\dot{v}_y, {}^b\dot{v}_z\}$ can be written as

$$\left.\begin{aligned} {}^b\dot{v}_x &\approx -g\sin\theta - \tfrac{k_1}{m}{}^b v_x \\ {}^b\dot{v}_x &\approx g\cos\theta\sin\phi - \tfrac{k_1}{m}{}^b v_y \end{aligned}\right\}, \tag{3}$$

where

$$k_1 = \lambda_1 \sum_{i=1}^{4} \omega_i.$$

In what follows, we assume that k_1 is a positive constant considering the fact that the summation of propeller rotational rates are fairly constant during smooth flight.

Inertial Sensors in Quadrotors

This article is concerned with the quadrotor state estimators based on inertial sensors and specifically with the accelerometers and the gyroscopes. For simplicity, we assume that a triad of the accelerometers and the gyroscopes are mounted at the center of mass of the quadrotor body. For both types of sensors, we adhere to standard MEMS error models [15].

The gyroscopes measure the instantaneous rotational rate of the body with respect to the inertial frame, and their measurements can be modeled independently of the equations of motion of the moving platform to which they are attached.

$$gi = \Omega_i + \beta_{gi} + w_{gi}, \tag{4}$$

$$\dot{\beta}_{gi} = -\frac{1}{\tau_{gi}}\beta_{gi} + w_{\beta gi}, \tag{5}$$

where β_{gi} is the bias of ith gyroscope and τ_{gi} is the time constant of ith gyroscope bias. w_{gi} and $w_{\beta gi}$ are zero-mean white Gaussian noise (WGN) terms.

In contrast, accelerometers measure a combination of inertial and gravitational acceleration, and their measurements can be expressed using the equations of motion governing the body they are mounted on. Perhaps one of the best example of the value of this strategy is the case of a triad of accelerometers mounted on a quadrotor platform. Denoting by $\tilde{a}_i$ the acceleration that would be measured by an ideal accelerometer, we combine the accelerometer measurement model with (2) to arrive at

$$\tilde{\mathbf{a}} = \dot{\mathbf{V}} - \mathbf{g} = -k_T \sum_{i=1}^{4} \omega_i^2 \mathbf{b}_3 - \lambda_1 \sum_{i=1}^{4} \omega_i \tilde{\mathbf{V}}, \tag{6}$$

which describes the readings obtained from an on-board triad of accelerometer, is unique to quadrotors, and is of critical importance to a state estimator in that context. As stated in the previous section, (6) shows that the accelerometers along the $\mathbf{b_1}$ and $\mathbf{b_2}$ coordinate axes are only sensitive to a force that is dependant on the projection of the quadrotor translational velocity onto the $\mathbf{b_1}$, $\mathbf{b_2}$ plane. Furthermore, the component of the gravitational acceleration in the body frame (which is typically large when compared to inertial accelerations of slow-moving vehicles) no longer influences the accelerometer measurement. In the next section, we will exploit this unique property to design a better state estimator for quadrotors.

Estimator Design

The goal here is to design a state estimator for the quadrotor, with regard to the dynamic and kinematic equations presented in the previous sections. For this, we propose a six-state extended Kalman filter (EKF)-based state estimator. The filter states are:

- ϕ, the roll angle in current orientation estimate
- θ, the pitch angle in current orientation estimate
- β_{gx}, the bias in X axis gyroscope
- β_{gy}, the bias in Y axis gyroscope
- ${}^b v_x$, the X velocity component of quadrotor in body frame
- ${}^b v_y$, the Y velocity component of quadrotor in body frame.

Process Model

The EKF process equations are formed by (1) and (3)–(5). Out of the three Euler angles, we can only estimate ϕ and θ, as the process and measurement equations are expressed in a form independent of the yaw angle ψ.

$$\left.\begin{aligned} \dot{\phi} &= (g_x - \beta_{gx} + w_{gx}) + \tan\theta\cos\phi\,(g_z - \beta_{gz}) \\ &\quad + \tan\theta\sin\phi\,(g_y - \beta_{gy} + w_{gy}) \\ \dot{\theta} &= \cos\phi\,(g_y - \beta_{gy} + w_{gy}) - \sin\phi\,(g_z - \beta_{gz}) \end{aligned}\right\}, \tag{7}$$

$$\left.\begin{aligned} \dot{\beta}_{gx} &= -\frac{1}{\tau_{gx}}\beta_{gx} + w_{\beta gx} \\ \dot{\beta}_{gy} &= -\frac{1}{\tau_{gy}}\beta_{gy} + w_{\beta gy} \end{aligned}\right\}, \tag{8}$$

$$\left.\begin{aligned} {}^b\dot{v}_x &= -g\sin\theta - \frac{k_1}{m}{}^b v_x + w_{\alpha x} \\ {}^b\dot{v}_y &= -g\cos\theta\sin\phi - \frac{k_1}{m}{}^b v_y + w_{\alpha y} \end{aligned}\right\}, \tag{9}$$

where $w_{\alpha x}$ and $w_{\alpha y}$ are WGN terms included to account for the model imperfections in (3).

Equations (7)–(9) together describe the process dynamics of the estimator. The resulting system can be represented as a nonlinear function of states, control inputs, and noise terms.

$$\dot{\mathbf{x}} = f(\mathbf{x}, \mathbf{u}, \mathbf{w}).$$

Measurement Model

The observations of the EKF are the measurements from the X and Y accelerometers, which are aligned with $\mathbf{b_1}$ and $\mathbf{b_2}$, respectively. Measurement equations can be easily derived from (6), after including accelerometer noise terms, which are assumed to be Gaussian.

$$\left.\begin{aligned} a_x &= -\frac{k_1}{m}{}^b v_x + w_{ax} \\ a_y &= -\frac{k_1}{m}{}^b v_y + w_{ay} \end{aligned}\right\}, \tag{10}$$

where a_x and a_y are, respectively, the measurements from the X and Y axis accelerometers on-board the quadrotor. Here we assume that accelerometer biases are random constant values, which can be compensated for, offline.

EKF Mechanization Equations

For the mechanization of the EKF, the discrete state-transition matrix A_k should be calculated. For this, we first calculate F, which is the Jacobian matrix of partial derivatives of f with respect to $\mathbf{x}$. Then, A_k is calculated by discretization of the Jacobian matrix:

$$F(t) = \left.\frac{\partial f(\mathbf{x}, \mathbf{u}, \mathbf{w})}{\partial \mathbf{x}}\right|_{\hat{\mathbf{x}}_k, \mathbf{u}_k}.$$

Discretization is performed with a truncated Taylor series approximation and a sample time of T_s, resulting in:

$$A_k = I + F(t)\,T_s.$$

In deriving the discrete process noise matrix Q_k, we assume that noise terms in (7) and (8) are uncorrelated with each other as well as with accelerometer noise terms:

$$\begin{aligned} \mathbf{w} &= [w_{gx} \;\; w_{gy} \;\; w_{\beta gx} \;\; w_{\beta gy} \;\; w_{\alpha x} \;\; w_{\alpha y}]^T \\ W(t) &= \mathrm{diag}\,[\sigma_{gx}^2 \;\; \sigma_{gy}^2 \;\; \sigma_{\beta gx}^2 \;\; \sigma_{\beta gy}^2 \;\; \sigma_{\alpha x}^2 \;\; \sigma_{\alpha y}^2] \\ Q(t) &= G(t)\,W(t)\,G^T(t). \end{aligned}$$

The first four terms of the $W(t)$ are the noise variances of the gyroscope sensors and their biases. These can be found by experimentation with actual sensors. The last two terms, which correspond to the uncertainty in (9), were approximated first and then fine tuned for optimum performance of the estimator. Also,

$$G(t) = \left.\frac{\partial f(\mathbf{x}, \mathbf{u}, \mathbf{w})}{\partial \mathbf{w}}\right|_{\hat{\mathbf{x}}_k, \mathbf{u}_k}.$$

Discretization of $Q(t)$ results in Q_k:

$$Q_k = \int_0^{T_s} A\,Q(\tau)\,A^T d\tau.$$

The measurement matrix H required for the EKF can be directly obtained from (10) as

Figure 5. The AR.Drone quadrotor used for our experiments.

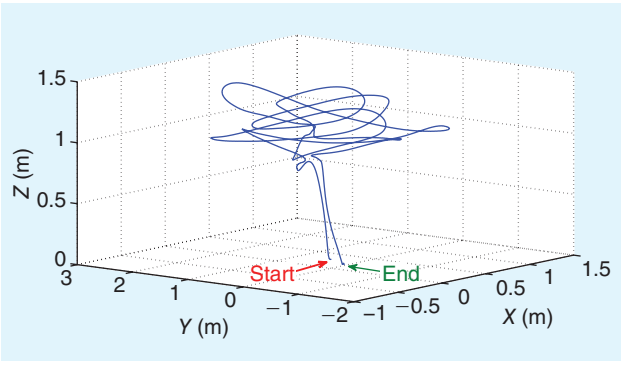

Figure 6. The 3-D flight path of the AR.Drone experiment.

$$H = \begin{bmatrix} 0 & 0 & 0 & 0 & -k_1/m & 0 \\ 0 & 0 & 0 & 0 & 0 & -k_1/m \end{bmatrix}.$$

Assuming uncorrelated errors in accelerometer measurements, measurement noise matrix R_k becomes diagonal, consisting only of the noise variances of the X and Y accelerometers:

$$R_k = \text{diag}\left[\sigma_{ax}^2 \;\; \sigma_{ay}^2\right].$$

For initialization, all states of the filter are set to zero, and their error covariances are set to small positive values reflecting the uncertainty in the initial estimate. With multiple experimental runs, it was found that changes of up to 100% in the initial values and the noise variances have negligible effect on filter performance. We attribute this robustness of the estimator to the linear measurement model and not-so-strong nonlinearities in the process equations.

The EKF state prediction was carried out with the use of a second-order Runge–Kutta integrator. The covariance projection, Kalman gain calculation, and state update and covariance update equations of the estimator take their standard forms as detailed in [16].

AR.Drone Quadrotor and the Experiments

The quadrotor platform used for the experiments presented in this article is the Parrot AR.Drone [17] (see Figure 5). The AR.Drone weighs about 420 g including the protective hull and has a flight time of about 10 min. Straight out of the box, the AR.Drone is an extremely stable quadrotor platform, and therefore it is an excellent platform for quadrotor-based research. It is equipped with a wide array of sensors, including a triad of accelerometers, a triad of gyroscopes, two cameras (one facing front and other facing down), and downward-pointing sonar sensors. All sensor data from the AR.Drone are wirelessly transmitted to a ground-station PC running either Windows or Linux. An open-source C application programming interface is provided, which can be easily extended to develop application on the ground station to process incoming sensor data and to send out control commands to the AR.Drone. It is also equipped with a preprogrammed closed-source attitude control system, which takes care of the low-level stabilization and control tasks, while providing users the ability to develop applications for higher-level navigational tasks.

It is desirable to have ground truth states trajectories for performance evaluation of the proposed estimator. Therefore, all our AR.Drone experiments were performed in a Vicon motion-capture environment. The Vicon motion-capture system uses a set of reflective markers rigidly attached to the quadrotor body, which are observed by eight fixed infrared cameras to directly compute the attitude and position of the quadrotor with respect to the Vicon coordinate frame.

In a typical experiment, the AR.Drone was manually piloted within the Vicon environment (approximately $6\text{ m} \times 4\text{ m} \times 3\text{ m}$) using a joystick attached to the ground-station computer. The inertial sensor data were continuously streamed to the ground-station computer at 200 Hz and were stored for postprocessing. Vicon-generated state estimated data were also stored in a separate PC. A MATLAB computing environment was used for postprocessing of both inertial and Vicon data.

A critical parameter that needs to be precomputed for the estimator is the rotor drag coefficient λ_1. Since a theoretical calculation of this parameter is a complex task, we resorted to an experimental estimation method. The basic methodology adopted here is to obtain the accelerometer measurements and ground truth velocity data of a few flight tests. A rough estimate of the parameter k_1 (which incorporates λ_1) can then be obtained by formulating (10) as a least-square problem. For the AR.Drone, the best estimate for the parameter k_1 was found to be 0.57. This parameter estimation task was run only once, and the derived k_1 value was used for all subsequent estimation tasks.

Experimental Results

During one experiment, the AR.Drone was manually operated within the Vicon environment, moving freely while keeping the height approximately constant. A 3-D trace of the path taken by the MAV in a typical experiment is shown in Figure 6. The results presented in the following sections are based on the data gathered from this experiment.

Figure 7 shows the attitude estimates of the proposed EKF together with the ground truth obtained from the Vicon system. For comparison, we have also plotted the attitude

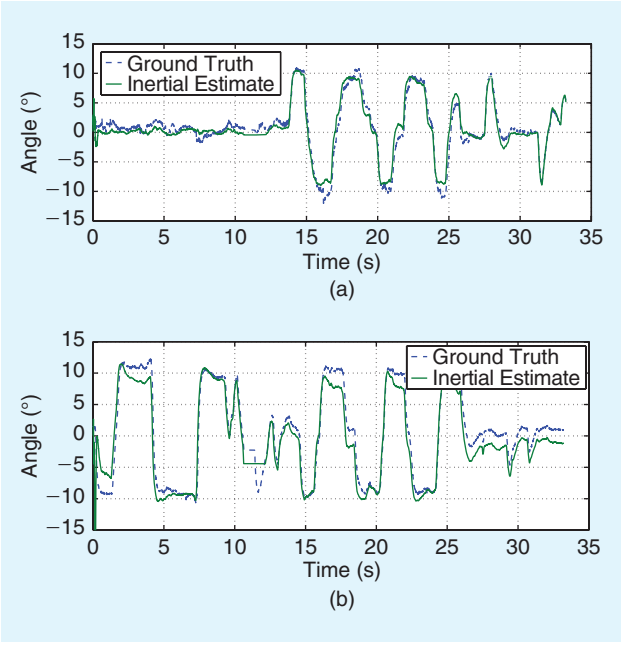

Figure 7. A comparison of ground truth and inertial attitude estimates of the AR.Drone: (a) roll angle (ϕ) and (b) pitch angle (θ).

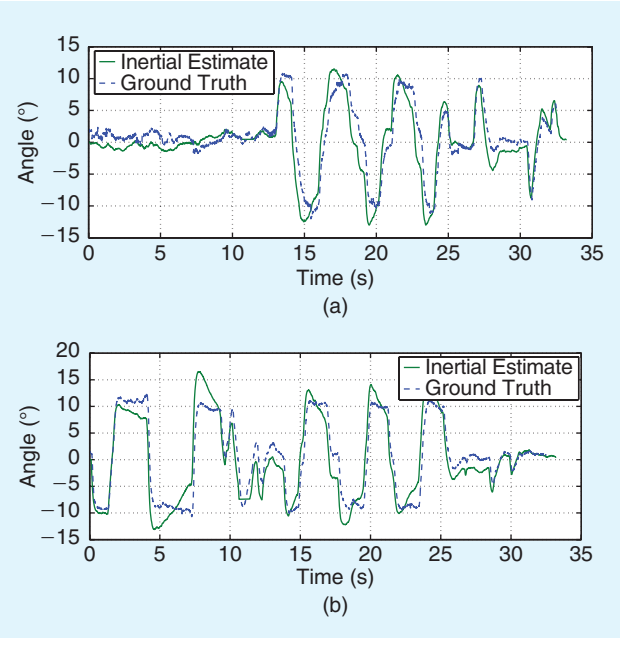

Figure 9. A comparison of ground truth and inertial attitude estimates of the AR.Drone, obtained from the generic estimator: (a) roll angle (ϕ) and (b) pitch angle (θ).

estimates from a generic estimator as detailed in [11] in Figure 9. It is important to note the improvement in the pitch estimate of the proposed estimator over the generic estimator. This improvement is more pronounced in places where the quadrotor changes its flight direction (e.g., around 4.6 and 7.8 s). During those intervals, the quadrotor undergoes high inertial accelerations, and the assumption that the accelerometer measurements are dominated by gravitational acceleration fails to hold. Therefore, generic attitude estimators based on this assumption produce erroneous results. As expected, the proposed EKF attitude estimates agree more with the ground truth because such an assumption is not utilized in that design. However, when the quadrotor is not undergoing considerable accelerations, the two attitude estimates converge, and the generic estimator can perform just as well as the proposed method.

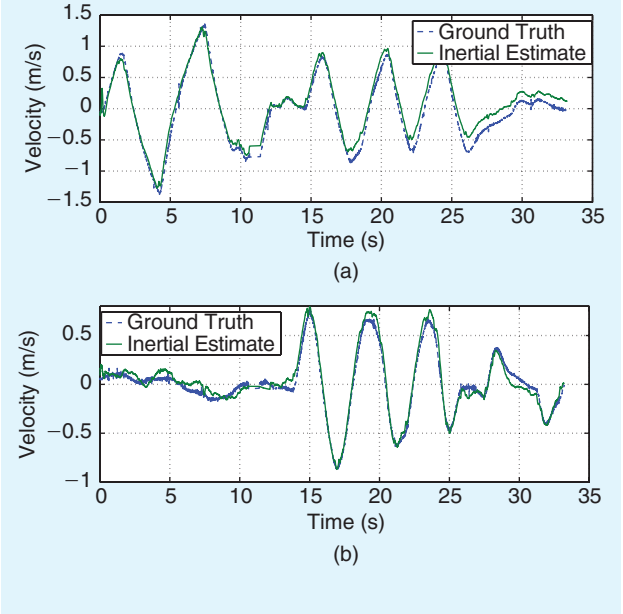

Figure 8. A comparison of ground truth and inertial velocity estimates of the AR.Drone: (a) X velocity (V_x) and (b) Y velocity (V_y).

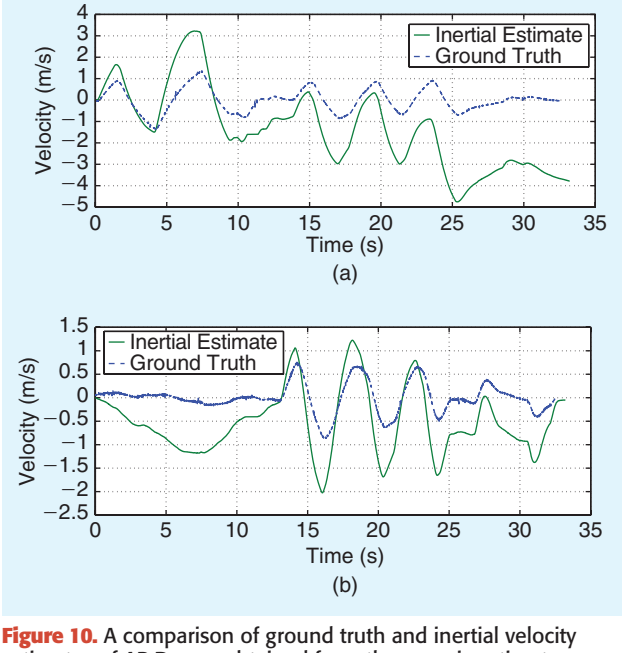

Figure 10. A comparison of ground truth and inertial velocity estimates of AR.Drone, obtained from the generic estimator: (a) X velocity (V_x) and (b) Y velocity (V_y).

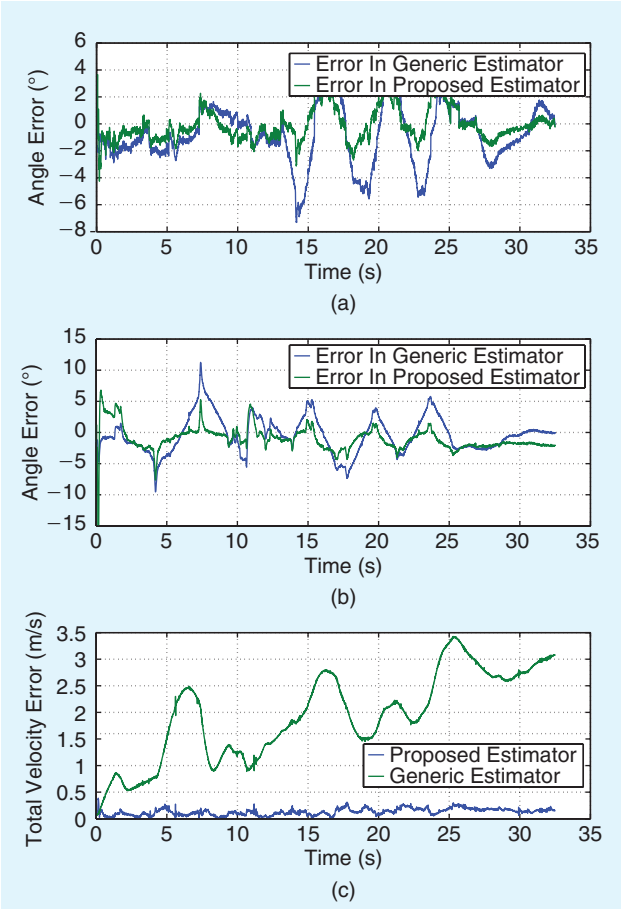

Figure 11. The estimation errors of both estimator designs: (a) roll angle (ϕ) estimation error, (b) pitch angle (θ) estimation error, and (c) total velocity estimation error.

Figure 11(a) and (b) presents a comparison between the errors in the roll and pitch attitude estimates of both the proposed EKF and the generic estimator. Even with the proposed EKF, unmodeled dynamics (such as displacement of accelerometer from the center of mass of the quadrotor) causes an increase in estimation error when the quadrotor undergoes large accelerations. But, overall, it is clear that the errors in the proposed design are considerably less than those of the generic design.

Figure 8 presents the velocity estimate from the proposed EKF together with the ground truth. Again for comparison, Figure 10 shows the velocity estimates in a generic design in which the velocity is estimated by integrating inertial accelerations calculated by compensating the accelerometer measurements for gravity. A comparison between the errors in velocity estimate obtained from the proposed estimator and the generic estimator is shown in Figure 11(c), where the total velocity error is the sum of the root square errors of both the X and Y axes. What is important to note is that the proposed strategy produces velocity estimates in which errors do not grow with time, but estimating velocity through direct integration of accelerations as implemented in the conventional design leads to a significant drift. As zero velocity updates, which can be used to correct this behavior in land vehicles, are no longer viable with an MAV without some deliberate control strategies, this points to a significant advantage of the estimator proposed in this article.

Conclusion

In this article, we presented a novel state estimator for quadrotor MAVs, where clear improvements in estimates stemming from the incorporation of quadrotor-specific dynamical constraints were demonstrated. Our design is based on an EKF and is capable of estimating both roll and pitch angles of the attitude, in addition to X and Y components of the body frame translational velocities within a bounded error. This estimator is applied to inertial data gathered from real-world flight experiments. The resulting attitude and velocity estimates obtained match closely with the ground truth and are drift free.

Before concluding the discussion on the estimator performance, we note that our design by itself is not a perfect solution to the problem of quadrotor state estimation. We believe that two key improvements need to be made to our design. First, an online estimation of the parameter λ_1 and accelerometer biases will improve estimation accuracy and ease the filter design process. Second, the estimation ψ angle and velocity ${}^b v_z$ will improve the autonomy of the quadrotor. Our current research focuses on these improvements.

In addition, we also expect to fuse the inertial information with exteroceptive sensors such as cameras and GPS. The two cameras in the AR.Drone makes it an ideal platform for visual simultaneous localization and mapping (SLAM). One key drawback in employing monocular SLAM for the MAVs is the unavailability of odometry for scale recovery. Another more obscure problem is the alignment of the camera with the MAV body frame. From a control theoretic perspective, orientation of the body frame is what matters, and the misalignment of camera and body frames can lead to poor control performance in a SLAM-only MAV state estimator. Both these problems can be solved by tightly integrating the estimation algorithm presented here with a monocular SLAM algorithm. We believe this to be an exciting research avenue.

Acknowledgments

This work was supported by the Centre for Intelligent Mechatronics Systems (CIMS), University of Technology, Sydney, Australia.

References

[1] D. Mellinger, N. Michael, and V. Kumar, "Trajectory generation and control for precise aggressive maneuvers with quadrotors," in *Proc. Int. Symp. Experimental Robotics*, Dec. 2010.

[2] D. Kingston and R. W. Beard, "Real-time attitude and position estimation for small UAVs using low-cost sensors," in *Proc. AIAA 3rd Unmanned Unlimited Tech. Conf.*, 2004, pp. 2004–6488.

[3] M. Achtelik, A. Bachrach, R. He, S. Prentice, and N. Roy, "Autonomous navigation and exploration of a quadrotor helicopter in GPS-denied indoor environments," in *Proc. Robotics: Science Systems Conf.*, June 2008.

[4] M. Bryson and S. Sukkarieh, "Building a robust implementation of bearing-only inertial slam for a UAV," *J. Field Robot., Special Issue SLAM Field*, vol. 24, nos. 1–2, pp. 113–143, 2007.

[5] C. N. Taylor, "Enabling navigation of MAVs through inertial, vision, and air pressure sensor fusion," in *Multisensor Fusion Integration Intelligent Systems* (Lecture Notes in Electrical Engineering), vol. 35. Berlin, Germany: Springer-Verlag, 2009, pp. 143–158.

[6] S. Ahrens, D. Levine, G. Andrews, and J. How, "Vision-based guidance and control of a hovering vehicle in unknown, GPS-denied environments," in *Proc. IEEE Int. Conf. Robotics Automation*, May 2009, pp. 2643–2648.

[7] S. Fux, "Development of a planar low cost inertial measurement unit for UAVs and MAVs," M.S thesis, Dept. Comput. Sci., Swiss Federal Inst. Technol., Zurich, Switzerland, 2008.

[8] G. Dissanayake, S. Sukkarieh, E. Nebot, and H. Whyte, "A new algorithm for the alignment of inertial measurement units without external observation for land vehicle applications," in *Proc. IEEE Int. Conf. Robotics Automation*, 1999, pp. 2274–2279.

[9] M. Tahk and J. Speyer, "Target tracking problems subject to kinematic constraints," *IEEE Trans. Autom. Control*, vol. 35, no. 3, pp. 324–326, 1990.

[10] N. S. Kumar and T. Jann, "Estimation of attitudes from a low-cost miniaturized inertial platform using Kalman filter-based sensor fusion algorithm," *Sadhana*, vol. 29, pp. 217–235, Apr. 2004.

[11] D. Abeywardena and S. Munasinghe, "Performance analysis of a Kalman filter based attitude estimator for a quad rotor UAV," in *Proc. Int. Congr. Ultra Modern Telecommunications Control Systems Workshops*, 2010, pp. 466–471.

[12] P. Martin and E. Salaun, "The true role of accelerometer feedback in quadrotor control," in *Proc. IEEE Int. Conf. Robotics Automation*, May 2010, pp. 1623–1629.

[13] R. Mahony, V. Kumar, and P. Corke, "Multirotor aerial vehicles: Modeling, estimation, and control of quadrotor," *IEEE Robot. Autom. Mag.*, vol. 19, no. 3, pp. 20–32, Sept. 2012.

[14] P. Bristeau, P. Martin, E. Salaun, and N. Petit, "The role of propeller aerodynamics in the model of a quadrotor UAV," in *Proc. European Control Conf.*, 2009, pp. 683–688.

[15] M. Park, "Error analysis and stochastic modeling of MEMS based inertial sensors for land vehicle navigation applications," M.S thesis, Dept. Geomatics Eng., Univ. Calgary, Calgary, AB, Canada, 2004.

[16] M. S. Grewal and A. P. Andrews, *Kalman Filtering: Theory and Practice Using Matlab*. New York: Wiley, 2001.

[17] Available: http://ardrone.parrot.com/parrot-ar-drone

Dinuka Abeywardena, Centre for Intelligent Mechatronic Systems, University of Technology, Sydney, NSW, Australia. E-mail: dinuka.abeywardena@uts.edu.au.

Sarath Kodagoda, Centre for Intelligent Mechatronic Systems, University of Technology, Sydney, NSW, Australia. E-mail: sarath.kodagoda@uts.edu.au.

Gamini Dissanayake, Centre for Intelligent Mechatronic Systems, University of Technology, Sydney, NSW, Australia. E-mail: gamini.dissanayake@uts.edu.au.

Rohan Munasinghe, Department of Electronic and Telecommunication Engineering, University of Moratuwa, Sri Lanka. E-mail: rohanm@uom.lk.